

Investigation of the Restoring Force Model of Through-tenon and Half-tenon of Timber with a Certain Level of Universality

Zhongwei Gao,^{a,b} Donghui Ma,^{a,c} Ziyi Wang,^{a,c} Xiaodong Guo,^{a,c,*} Shidong Fang,^a and Zhitao Fei^a

A restoring force model of through-tenon and half-tenon joints was studied with a certain level of universality. To address the differences among data collected under different test conditions, test data collected *via* through-tenon and half-tenon joints were counted and fitted, and their similarities were then generalized. To better simulate the gap and stiffness degradation between the through-tenon and half-tenon joints, the skeleton curves frameworks were simplified into four phases, namely sliding, elastic, yielding, and failure. The normalized control parameters collected through the characteristics of the framework of through-tenon and half-tenon joints, as well as the different coefficients of strength degradation and stiffness degradation were calculated. The hysteretic rules of the restoring force model of through-tenon and half-tenon joints were developed. Through case study, the results show that the MAPE (mean absolute percentage error) and R^2 (coefficient of determination) of experimental data in the references and simulated data of through-tenon are respectively 12.570% and 0.735, while those of half-tenon are respectively 11.763% and 0.772; and the restoring force model of through-tenon and half-tenon joints being constructed had a certain level of universality. The results demonstrated that the construction of refined finite element analysis model of Chinese ancient timber architectures can be simplified to a certain extent to meet the pressing time for seismic performance analysis of many ancient timber architectures. It provides researchers with an innovative pathway to enhance the efficiency of seismic performance analysis of ancient timber architectures.

Keywords: Through-tenon joints; Half-tenon joints; Universal restoring force model; Simplified skeleton curve framework; Strengthened degeneration; Stiffness degeneration

Contact information: a: Institute of Earthquake Resistance and Disaster Reduction, Beijing University of Technology, Beijing 100124, China; b: Sichuan Institute of Building Research, Chengdu 610081, China; c: Key Scientific Research Base of Safety Assessment and Disaster Mitigation for Traditional Timber Structure (Beijing University of Technology), State Administration for Cultural Heritage, Beijing 100124, China; *Corresponding author: gxd@bjut.edu.cn

INTRODUCTION

Chinese ancient timber architectures have important cultural and historic heritage values. The studies of Chinese ancient timber architectures provide the protections of their national cultural and historical heritage values, as they are unique and unrenewable resources.

In the centuries of use of Chinese ancient timber architectures, due to the joint effect of various factors, such as material aging, environmental erosion, component defects, long-

term effect of load, fatigue effect, natural disasters, and some human factors such as improper protection in the later period, damage accumulation and resistance deterioration of the structural system is inevitable. This may result in partial or total loss of function of many components. Their anti-disaster ability is poor, and once a disaster occurs, the consequences will be serious. For example, 24 national, 78 provincial, 157 municipal and county-level cultural protection units, and 7 cultural relic sites were damaged to various degrees during the M7.0 earthquake in Lushan County, Sichuan Province on April 20th, 2013. Among all the damaged building, 149 are ancient architectures, accounting for 56% of the total (Pan *et al.* 2014).

Therefore, it is important to study the seismic performance of Chinese ancient timber architectures. Currently, the main research methods include experimental research and numerical simulation. For example, Yang *et al.* (2021) conducted experiments and numerical simulation to study the mechanical performance of plinths under loading of Chinese ancient timber architectures and developed the simplified model of rotational stiffness of the plinth's joints. Eckelman *et al.* (2008) also tested the mortise-tenon joints and studied the influence of flexural performance on the joints at the 5% yielding point. Moreover, Zhao *et al.* (2010) studied the friction effect on the energy dissipation capacity of mortise of six groups of mortise-tenon joints. They found that the friction has a limited effect on the failure mode, bearing capacity, ductility of through-tenon, and dovetail tenons joints.

In the study of Zhou and Yan (2011), the method of combining theoretical calculation and finite element simulation was used to study the reinforcement method of a wooden beam in Taihe Hall of the Forbidden City. Xu and Qiu (2011) carried out experimental research on the failure mode, hysteretic curve, and other properties of dovetail tenon joints. Their experimental results showed that the dovetail tenon joint has good deformation ability. Sakata *et al.* (2012) conducted bending tests on mortise-tenon joints, studied their bending performance, and developed the bending criteria and simplified equations of mortise-tenon joints.

Johanides *et al.* (2021) analyzed the rotational stiffness of wood frame joints to replace common fasteners with more modern fasteners. Cui *et al.* (2020) did a shaking table test on the Chinese column and tie wooden construction before and after the restoration. They found that the Chinese column and tie wooden construction houses have stable energy dissipation mechanism and excellent seismic performance. Amaruddin *et al.* (2013) simulated the tenon-mortise joints of dowels by using the finite element method and analyzed the mechanical properties of the joints under tension.

Considering the influence of different tenon pulling degrees, Song (2014) studied the seismic performance, such as the hysteretic curve and skeleton curve, of the through-tenon, half-tenon, and dovetail tenon. The experimental results of Song's studies showed that the hysteresis curve of each timber frame changes to different degrees in the horizontal reciprocating loading process, *i.e.*, shuttle shape first, then reverse S-shape, and finally anti-Z-shape. The effect of "pinching" was throughout the process. Chen *et al.* (2020) also used artificial damage simulation to study the influence of the degree of decay on the seismic performance of ancient timber architectures connected by one-way straight tenon. The findings showed that the damage depth of mortise has great effects on the seismic performance of frame structure.

Xie *et al.* (2020) conducted an experimental study on the lateral performance of traditional Chinese timber frames strengthened with shape memory alloy. They found that

under the condition of large displacement, the strengthened specimens' lateral bearing capacity, stiffness, and energy consumption were significantly improved, even exceeding the undamaged level. Aejaz *et al.* (2020) also conducted an experimental study on the mechanical properties of full-scale timber structure joints, such as dovetail tenon and half-tenon, with adhesive and pure nail connection under tensile load. Their results indicated that adding adhesive is an effective and economical method to improve the properties of various dowels connections under tensile load. However, the feasibility of using such measures to reinforce the ancient architectures still needs further discussion. In addition, the hysteretic curve and skeleton curve of straight tenon were studied by Xie *et al.* (2015a), and they found that the failure modes of the straight tenon joints come from the extrusion deformation of the mortise and tenon.

Gao *et al.* (2015) studied the effect of friction between the contact surfaces of tenon-mortise joints on the seismic energy dissipation capacity of tenon-mortise joints. Their experimental results showed that friction has a limited effect on the failure mode, bearing capacity, and ductility of through-tenon and dovetail tenon joints. Chen *et al.* (2017) conducted a case study on tenon joints of an ancient building in Yangzhou and undertook a static cyclic loading test to analyze the bending resistance of the original tenon-mortise joints. Qu *et al.* (2020) investigated the seismic performance of columns and tie wooden constructions and found that the masonry filler has the largest lateral force resistance. At the same time, the timber frame can withstand large lateral displacement without losing vertical stability.

Recently, Shi *et al.* (2020) conducted a full-scale model test on the horizontal hysteretic behavior of timber frame with tenon-mortise connection, and their findings showed that the timber frame is a self-centering structure with high ductility and weak hysteretic energy consumption. It was also found by Shi *et al.* (2020) that its rotational deformation is mainly caused by the rotation of columns. Huan *et al.* (2019) studied the failure mode, skeleton curve and other seismic performance parameters of through-tenon joints. They found that the hysteretic curve of through-tenon joints has an obvious pinch effect, and there is friction sliding between tenon-mortise joints.

The influence of lateral tightness of tenon-mortise joints on the seismic performance of through-tenon joints was studied by Su *et al.* (2020). The tightness was found to have a great impact on the energy consumption, ultimate bearing capacity, initial stiffness, and ductility of the joints. They concluded that the closer the tenon-mortise joints are, the more obvious the brittle characteristics are. Wan *et al.* (2020) also established the finite element model of a typical Chinese traditional timber frame and conducted a parameter analysis. It was found the results are consistent with the analytical distribution. The rocking characteristics of free-standing columns supported by the superstructure were then studied by Gao *et al.* (2020). The results showed that most of these traditional timber structures have good seismic capacity and can resist horizontal excitation. A total of 23 unidirectional straight tenon joints were made by Li *et al.* (2019) to conduct low cycle reversed tests to investigate the mechanical properties of straight tenon joints with different damage degrees. Xue *et al.* (2019) carried out low-cyclic reversed loading tests on through-tenon and dovetail tenon joints to analyze the seismic performance of tenon-mortise joints as well. Xie *et al.* (2019) further studied Chinese timber frame specimens with different types of masonry infilled walls, and they found that the masonry infilled wall enhances the seismic performance of the structure.

Ma *et al.* (2019) developed a theoretical force formula of the pull-out moment of the tenon-mortise joint by analyzing the stress distribution of the tenon-mortise joint after pull-out failure. They studied the intact joints and different damaged degree of timber frame and found that the moment bearing capacity from the test and the simulation are consistent with each other. Moreover, comparing with the intact joints, the bearing capacity and energy dissipation capacity of the joints after pull-out failure do not change. They also found the friction between tenon-mortises is the main source of the bending bearing capacity and energy dissipation capacity. Additionally, Sha *et al.* (2019) conducted a finite element simulation analysis on the damage forms of tenon-mortise joints of traditional Chinese timber structures under cyclic loading. The damage of joints had adverse effects on the lateral performance of timber frames, and these damages weakened the stiffness and energy dissipation capacity of timber frames.

Zhang *et al.* (2019) carried out a fast nonlinear analysis on the energy consumption of column base sliding, tenon-mortise connection, and bucket arch. The results were consistent with the previous shaking table test results (Zhang *et al.* 2011). Another study by Guo *et al.* (2021) was conducted on the lateral performance of traditional Chinese timber frames. The vertical load and column height had a significant impact on the lateral performance of traditional Chinese timber frames. Meng *et al.* (2019) studied the seismic response of an ancient timber architecture model with a column framework layer and bucket arch layer. The ultimate load state of the timber structure is mainly controlled by the lateral displacement of the column framework layer. Moreover, the hysteretic and stiffness properties of the column framework layer are similar to the whole structure; the stiffness of the bucket arch layer, not degenerated, is much higher than that of the column framework layer.

Finally, Huang *et al.* (2018) investigated the ultimate bearing capacity, stiffness, and damage characteristics of three kinds of column and tie wooden constructions. They found that the column and tie wooden construction has good deformation capacity and energy dissipation capacity, but poor ultimate bearing capacity and stiffness. Han *et al.* (2020) researched the bending moment-rotational angle hysteretic curves, moment-rotational angle skeleton curves, ductility, stiffness degradation, energy dissipation capacity, slippages between the wooden column and the plinth, and the damage of the column foot tenons. The test results showed that the rotation of the column foot tenon improves the energy dissipation capacity of the wooden column. With the increase of the angle of the column base, the column foot tenon has different degrees of damage. Different sizes of column foot tenon has their own advantages and hysteretic behavior.

The above literature shows that experimental research and numerical simulation of the seismic performance of ancient timber architectures have been conducted extensively, and some significant development has been made. However, there are still some areas needing exploration and study. One, the experimental research results of ancient timber architectures were generalized from some specific test data. Only when the material parameters and joint size were completely aligned with the test conditions, the relevant results would show significant results, limiting the scope of its use and the levels of generalizations to other conditions. Two, the finite element analysis software has no matching constitutive relations with Chinese ancient timber architectures. Thus, the reliability and credibility of the calculation results are difficult to be guaranteed. This study focused on the restoring force model of through-tenon and half-tenon joints with a certain level of universality.

This paper used the statistical analysis of the experimental data of through-tenon and half-tenon joints/timber frames to develop a universal restoring force model of through-tenon and half-tenon joints. This model provides an innovative pathway to simplify the process of the construction of refined finite element analysis model of Chinese ancient timber architectures, especially for the circumstances when the quantities of ancient timber architectures are large and the time for seismic performance analysis is pressing. Further, it can also enhance the efficiency of seismic performance analysis of ancient timber architectures.

SIMULATION

Methods

The anisotropic of timber mechanical properties and the mechanical properties of the same tree species have their own discrete characteristics. Therefore, the test conditions developed for prototype structure, scale ratio, tree species, and timber mechanical properties were different. To address these differences, the collected test data of through-tenon and half-tenon joints were counted and fitted. By using a consistent principle, Eq. 1 was used to normalize the test data, to consider the timber column diameter and timber elasticity modulus,

$$\bar{K} = (K_t \cdot \frac{D_{1000}}{D_t}) \cdot \frac{1}{E_t} \quad (1)$$

where \bar{K} is the stiffness (N/mm*GPa) of through-tenon and half-tenon joints after normalization, K_t is the stiffness (N/mm) of through-tenon and half-tenon joints calculated by the test model. Parameter D_{1000} is the diameter of the timber column, which is unified taken as 1000 mm. Parameter D_t is the (mm) of the timber column, and E_t is the timber elasticity modulus (GPa) in the test model.

The principal rules shall be used before employing \bar{K} , and only after converting timber column diameter and timber elasticity modulus of the actual research objects. The conversion relationship is shown as Eq. 2,

$$K_{ei} = \left(\bar{K}_i \cdot \frac{D_e}{D_{1000}} \right) E_e = \frac{\bar{K}_i D_e E_e}{D_{1000}} \quad (2)$$

where K_{ei} is the stiffness of the i -stage of the actual research object; \bar{K}_i is the normalized stiffness (N/mm) of the i -stage obtained from Eq. 1; parameter D_e is the timber column diameter (mm) of through-tenon and half-tenon joints of the actual research object in mm; and parameter E_e is the timber elastic modulus (GPa) of the through-tenon joints of the actual research object.

Construction of Restoring Force Model of Through-tenon and half-tenon Joints

The through-tenon is also called silver ingot tenon and big head tenon. The shape of the tenon looks like a trapezoid; that is, the near end of the tenon is narrow and the far end is broad, like a big head (Fig. 1). The shape characteristics of the tenon ensure it has an excellent anti-pulling performance. It can effectively prevent the tenon from being pulled out. However, the section of the near end of through-tenon is small, making the

shear-bearing capacity of the through-tenon worse than the straight tenon. Among all tenon-mortise joints, the bonding strength of the through-tenon joint is the largest under tensile stress (Huan *et al.* 2019).

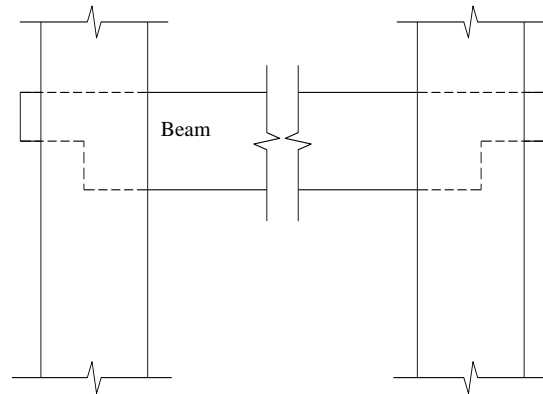


Fig. 1. Schematic diagram of through-tenon structure

Half-tenon is mainly used for interpenetrating members such as the interpenetrating tie beam and “Baotou” beam. The length of the half-tenon is about half of the through-tenon, and it no longer penetrates the timber column. Figure 2 shows the structure of the half-tenon. The tensile, bending, and shear-bearing properties of the half-tenon are similar to those of the through-tenon, but the resistance performance of the half-tenon is worse than that of the through-tenon. The tenon is easier to be pulled out. This explains why there is often replacement timber under the beam (tie beam) in carpentry work. The construction of the restoring force of the half-tenon joint helps to address the lack of the corresponding constitutive relation in the finite element analysis software (Ansys, ANSYS, Inc., 19.2, Pittsburgh, PA, USA), and provides technical support for the seismic performance evaluation, reinforcement, and repair of the ancient timber architectures.

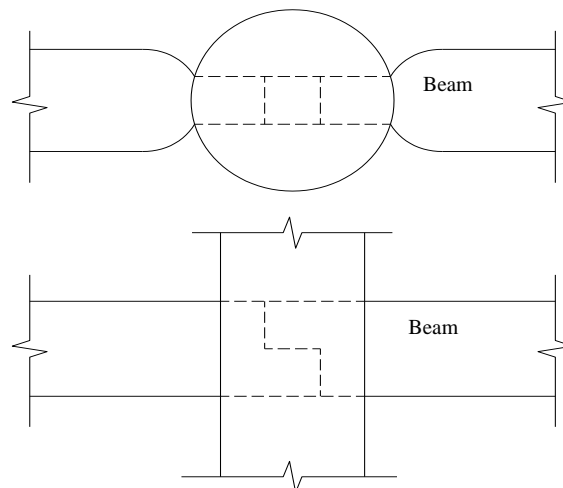


Fig. 2. Schematic diagram of half-tenon structure

Simplification of Skeleton Curves

The M - θ skeleton curve of tenon-mortise joints can be simplified into three phases (sliding, strengthening, and limitation) (Xu and Qiu 2011), or four phases (sliding, elasticity, yield, and failure) (Zhou *et al.* 2010). In order to better simulate the gap and stiffness degeneration between the through-tenon and half-tenon joints, the M - θ skeleton curve of the through-tenon and half-tenon joints is simplified into four phases, including sliding, elasticity, yield, and failure (Fig. 3).

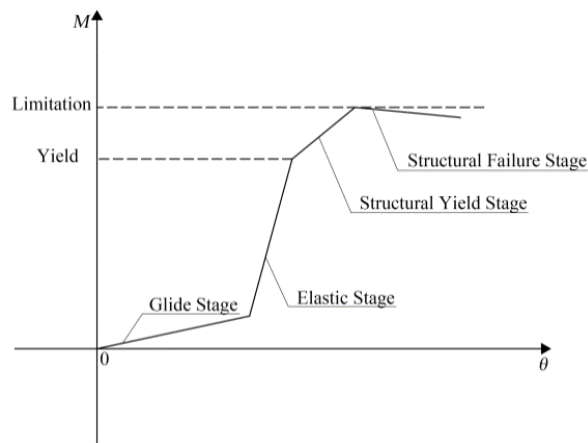


Fig. 3. M - θ skeleton curve

Hysteretic Rules

The hysteretic rules of through-tenon and half-tenon joints are associated with loading (unloading) and the state of joints. The hysteretic rules of through-tenon and half-tenon joints are defined, and the restoring force curve is shown in Fig. 4.

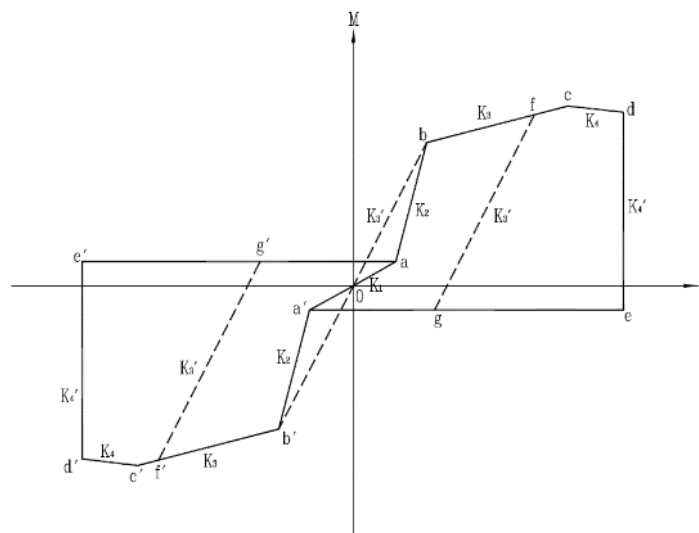


Fig. 4. The restoring force model of through-tenons joints and half-tenon joints

There is no plastic deformation and failure in the sliding and elasticity phase of the tenon-mortise members when the loading of the joints does not go beyond the yield strength. Thus, the stiffness degeneration is not considered during unloading in the sliding and elasticity phase. Figure 4 shows there are a positive (negative) loading (unloading) hysteretic path returns along the original path $b'-a'-0-a-b$. During the plastic development phase, the loading stiffness degenerates to K_3 , the unloading stiffness is K'_3 , and the stiffness of K'_3 is between K_1 and K_2 . The forward loading and unloading hysteretic path follows $0-a-b-f-g$ (Fig. 4). Figure 4 also shows the reverse loading, and the hysteretic unloading path follows $0-a'-b'-f'-g'$. During the failure phase, the loading stiffness degenerates to K_4 , and the unloading stiffness is K'_4 . It can be seen that $K'_4 \approx 0$; the forward loading and unloading hysteretic path follows $0-a-b-c-d-e$, and the reverse loading and hysteretic unloading path follows $0-a'-b'-c'-d'-e'$ (Fig. 4).

Determination of Characteristic Parameters of Skeleton Curve of Through-tenon and Half-tenon Joints

Statistics of control parameters at each characteristic point

The present study analyzed the 21 groups of through-tenon and 17 groups of half-tenon test data (Zhao *et al.* 2010; Chun *et al.* 2011; Song 2014; Gao *et al.* 2015; Xie *et al.* 2015b; Chun *et al.* 2016; Huan *et al.* 2019; Su *et al.* 2020) through the control parameters of each characteristic point of the skeleton curve of through-tenon joints. Table 1 presents an overview of a norm table of parameters at each control point of the skeleton curve of through-tenon joints. In Table 1, \bar{k}_i represents the norm stiffness of each stage, with the unit of N/mm^*GPa ; Δ_{ui} represents the story drift angle.

Table 1. Norm Table of Parameters of Each Control Point of the Skeleton Curve of Through-Tenon and Half-Tenon

State	Through-tenon Joints		Half-tenon Joints	
	\bar{k}_i (N/mm*GPa)	Δ_{ui}	\bar{k}_i (N/mm*GPa)	Δ_{ui}
Sliding	3.782083	1/297	2.050534	1/362
Elastic	36.704632	1/94	19.894090	1/117
Yielding	5.912254	1/28	2.435622	1/32
Failure	-3.525824	1/11	-1.596407	1/13

Statistics of strength and stiffness degeneration coefficient

Under the same loading conditions, it was found the bearing capacity of the members constantly decreased, while the controlled displacement increased when loading times increased during the plastic phase. That is, there were strength degeneration and stiffness degeneration during the plastic phase. Twenty groups of through-tenon and half-tenon test data were analyzed (Zhao *et al.* 2010; Chun *et al.* 2011; Song 2014; Gao *et al.* 2015; Xie *et al.* 2015b; Chun *et al.* 2016; Huan *et al.* 2019; Su *et al.* 2020). Table 2 presents the strength and stiffness degeneration coefficient of through-tenon and half-tenon joints.

Table 2. Summary of Strength Degradation Coefficient (a) and Stiffness Degradation Coefficient (b)

State	Through-tenon Joints		Half-tenon Joints	
	a	b	a	b
Sliding	0.9549	0.9373	0.9220	0.9418
Elastic	0.8726	0.8417	0.8622	0.8532
Yielding	0.7361	0.7601	0.6619	0.7244
Failure	0.6439	0.5862	0.5214	0.4637

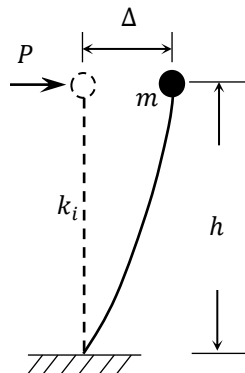
Case Study

This case study used the parameters of through-tenon (Sui *et al.* 2010) and half-tenon joints (Xie *et al.* 2015a) to develop the restoring force model. The elastic modulus of timber is 8.111 GPa, and the column diameters of through-tenon and half-tenon joints were 210 mm and 140 mm, respectively. According to Table 1, the control parameters at each characteristic point of the restoring force model of the through-tenon and half-tenon joints were calculated, respectively, as shown in Table 3. Moreover, the strength and stiffness degeneration coefficients were determined in Table 2. The finite element software OpenSees (University of California, Berkeley, OpenSees3.2.1, Berkeley, CA, USA) was then used to perform Push-over analysis on the calculated through-tenon and half-tenon joints.

Table 3. Parameters of Control Points of Through-Tenon and Half-Tenon Skeleton Curve

Stage	Through-tenon		Half-tenon	
	k_i (N/mm)	Δ_{ui}	k_i (N/mm)	Δ_{ui}
Sliding	6.442060	1/297	2.328463	1/362
Elastic	62.519367	1/94	22.590535	1/117
Yielding	10.070401	1/28	2.765746	1/32
Failure	-6.005571	1/11	-1.812784	1/13

According to the data in Tables 2 and 3, the through-tenon and half-tenon are simplified as a single-degree-of-freedom system, as shown in Fig. 5. The parameters m and h are both valued by Sui *et al.* (2010) and Xie *et al.* (2015a). That is, the mass m of through-tenon and half-tenon are respectively 2040 and 612.2 kg; the height h of them are respectively 1.7 and 0.8 m, while the vertical loads of them are respectively 20 and 6 kN. The parameter k_i is valued by referring to Table 3; P represents the horizontal thrust applied, and Δ is the horizontal lateral displacement under horizontal thrust P .

**Fig. 5.** single-degree-of-freedom system

RESULTS

According to the single-degree-of-freedom system shown in Fig. 5, the Push-over analysis of the hysteretic curves of the through-tenon and half-tenon joints from the finite element software OpenSees are shown in Figs. 6 and 7, respectively.

Compared with the elastic, yield and failure stages, the slip stage is relatively short; the slip stage in Figs. 6 and 7 is not obvious. Besides, Stage 1 ~ Stage 3 in Figs. 6 and 7 correspond to elastic, yield, and failure stage, respectively.

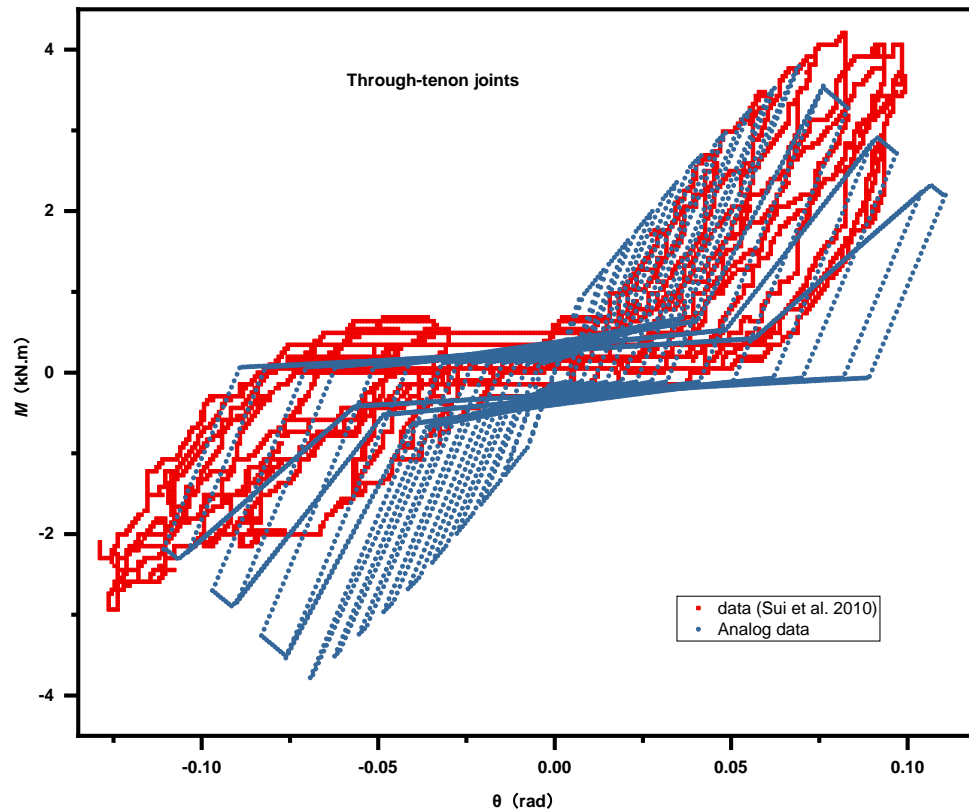


Fig. 6. Comparison of calculation results and test results

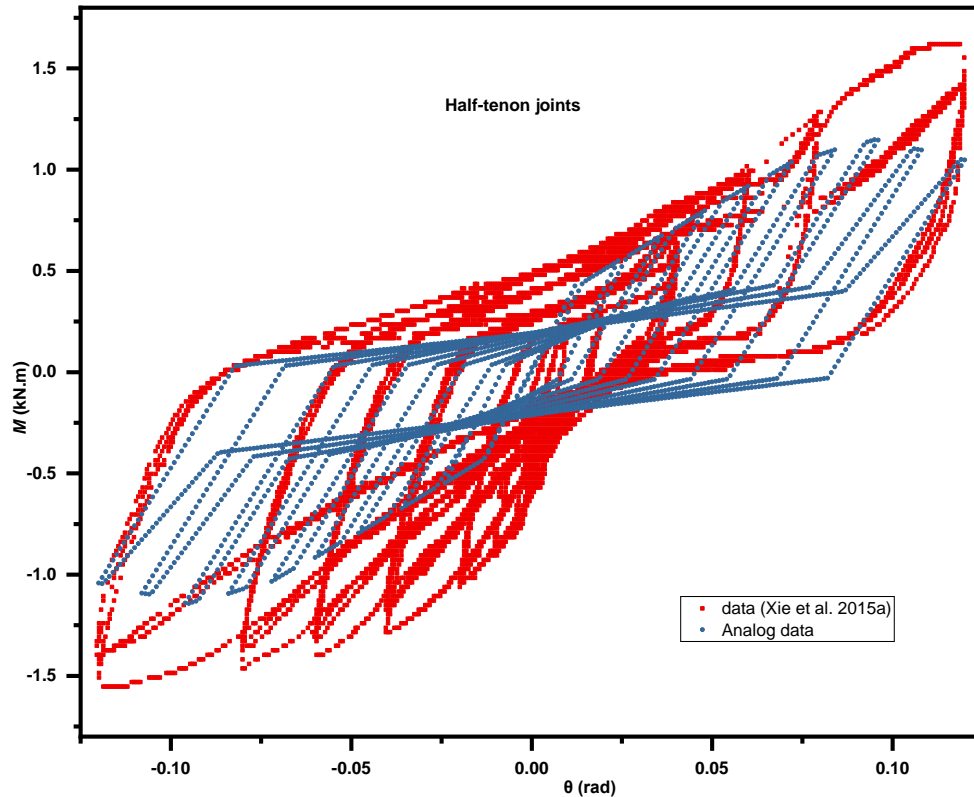


Fig. 7. Comparison of calculation results and test results

The calculation results show that:

- (1) The shape and changing trend of the simulated hysteretic curve was consistent with that of the actual hysteretic curve.
- (2) The ratios of the envelope area of the hysteretic curve obtained through simulation calculation (S_s) and the envelope area of the hysteretic curve obtained by test (S_t) were 1.3063 (S_s/S_t of through-tenon), and 1.2209 (S_s/S_t of half-tenon).
- (3) Comparison of the ultimate strength calculated by simulation with that in references (Sui *et al.* 2010 and Xie *et al.* 2015a) is shown in Table 4.

Table 4. Comparison of the Ultimate Strength Calculated by Simulation with that in References

Joint Type	Ratio of Average	MAPE	R ²
Through-tenon	1.141	12.570%	0.735
Half-tenon	1.127	11.763%	0.772

- (4) Different from the symmetrical hysteretic curve (Sui *et al.* 2010) or asymmetrical hysteretic curve (Xie *et al.* 2015a), the hysteretic curve using the restoring force model in this study had some degree of symmetry, but it was not completely symmetrical.

DISCUSSION

There was a margin of error in the ultimate strength of through-tenon and half-tenon joints during each phase calculated by the restoring force model with the actual data in literature (Sui *et al.* 2010; Xie *et al.* 2015a). There are two main reasons: on the one hand, there were great differences in the prototype structure, scale ratio, tree species, wood mechanical properties, and other test conditions, so the experimental data in the references used for statistics has certain discreteness. There were still some deviations of \bar{K}_i , joints strength degradation coefficient a and stiffness degradation coefficient b obtained through the statistic of the data above by using the similarity principle. On the other hand, the deviation is caused by simplifying the simulation model; including the simplification of skeleton curve, hysteresis rule, and finite element model and so on. In addition, the envelope area ratio of the hysteresis curve and the average ratio of the ultimate strength as well as MAPE between the simulation data and the experimental data in the references are all small, and R^2 is acceptable. Thus, the margin of error is acceptable in a simple calculation.

The hysteretic curves represent the accumulated loading, the degeneration of strength, and stiffness. They are calculated by using simulation, which can reflect the "pinch" effect of the calculated hysteretic curves of through-tenon and half-tenon joints.

The actual hysteretic curve is symmetrical because the connection structure of the through-tenon joints have more uniform forward and reverse forces than those of the half-tenon joints. However, it is not completely symmetrical according to the hysteretic curve calculated by the restoring force model. The actual reverse hysteretic curve is not symmetrical (Xie *et al.* 2015a), which is due to two reasons. One, the restoring force model of through-tenon and half-tenon joints developed in this paper had symmetry itself; two, the actual test data were being affected by the anisotropy of mechanical properties of timber materials and the material properties with certain discreteness as well as the compaction degree of tenon-mortise.

The parameters in Tables 1 and 2 were all obtained from statistical analysis of the data in references (Zhao *et al.* 2010; Chun *et al.* 2011; Song 2014; Gao *et al.* 2015; Xie *et al.* 2015a,b; Chun *et al.* 2016; Huan *et al.* 2019; Su *et al.* 2020). The data for case verification was converted from the relevant data in references (Sui *et al.* 2010 and Xie *et al.* 2015a) by using Eq. (2), that is, the data used for case verification did not participate in the statistics of the parameters in Tables 1 and 2. The comparative analysis shows that the error range between the simulated data and the experimental data in the references is acceptable. In summary, based on the statistical analysis of the relevant experimental results of through-tenon and half-tenon joints, the restoring force model of through-tenon and half-tenon joints developed in this paper can be generalized into a certain degree of universality.

CONCLUSIONS

The skeleton curve of the restoring force model of the through-tenon and half-tenon joints is simplified into four phases: sliding, elasticity, yield, and failure; and the hysteretic rules of the restoring force model of the through-tenon and half-tenon joints were formulated. Based on the principle of similarity, the characteristic parameters of skeleton

curves of through-tenon and half-tenon joints were calculated with the norm data collected from the relevant experiments. The finite element software was used to analyze the relevant test data and the following conclusions are drawn:

1. The restoring force model of through-tenon and half-tenon joints can represent the hysteretic behavior of through-tenon and half-tenon joints.
2. Using the method of timber column diameter and timber elastic modulus, the margin of error in the results caused by different prototype structure, scale ratio, tree species, and timber mechanical properties can be accepted to a certain extent.
3. The restoring force model of through-tenon and half-tenon joints developed in this paper can be generalized into a certain degree of universality. Thus, this restoring force model can be used to simplify the construction of a refined finite element analysis model of Chinese ancient timber architectures. In addition, it also provides a new pathway to enhance the efficiency of seismic performance analysis of Chinese ancient timber architectures.
4. This paper has its limitations. Due to the limited relevant test data collection, the restoring force model of through-tenon and half-tenon joints will be developed further in future research.

ACKNOWLEDGMENTS

The authors are grateful for the support of Beijing Municipal Commission of Education-Municipal Natural Science Joint Foundation: “Research on Seismic Performance Evaluation of Beijing Ancient Timber Buildings Based on Value and damage Characteristics” (No. KZ202010005012).

REFERENCES CITED

- Aejaz, S. A., Dar, A. R., and Bhat, J. A. (2020). “Structural performance of timber frame joints - Full scale tests and numerical validation,” *Structural Engineering and Mechanics* 74(4), 457-470. DOI: 10.12989/sem.2020.74. 4.457
- Amaruddin, H. I., Hassan, R., Amin, N. M., and Malek, N. J. A. (2013). “Finite element model of mortise and tenon joint fastened with wood dowel using kempas species,” in: *InCIEC 2013*, Springer Singapore, Sarawak, Malaysia, pp. 3-14. DOI: 10.1007/978-981-4585-02-6_1
- Chen, L. K., Li, S. C., King, W. S., Jiang, L. Z., and Li, Q. J. (2020). “How the decayed straight mortise-tenon joints influence the seismic performance of ancient timber building? Evidence from experiment scenarios of the benchmark wood frames,” *Engineering Failure Analysis* 116, Article ID: 104685. DOI: 10.1016/j.engfailanal.2020.104685
- Chen, L. K., Li, S. C., Wang, Y. T., Zhao, Y. J., Zhang, M., Song, X. Y., Li, X. W., Wu, T., and Jiang, L. Z. (2017). “Experimental study on the seismic behavior of mortise-tenon joints of the ancient timbers,” *Structural Engineering International* 27(4), 512-519. DOI: 10.2749/222137917X14881937844720

- Chun, Q., Le, Z., and Pan, J. W. (2011). "Experimental study on seismic characteristics of typical mortise tenon joints of Chinese southern traditional timber frame buildings," *Science China* 41(9), 1153-1160. DOI: 10.1007/s11431-011-4448-3
- Chun, Q., Pan, J. W., and Han, Y. D. (2016). "Research on mechanical properties of ban mortise-tenon joint of the traditional timber buildings in the south Yangtze River regions," *Journal of Hunan University (Natural Sciences)* 43(1), 124-131. DOI: 10.3969/j.issn.0258-2724.2016.05.007
- Cui, C. Y., Li, Z. H., Chen, Y., and Zhu, Q. Y. (2020). "Seismic performance and repair of Chuan-dou timber framed masonry building," *Engineering Failure Analysis* 118, Article ID 104941, DOI: 10.1016/j.engfailanal.2020.104941
- Eckelman, C., Haviarova, E., and Akcay, H. (2008). "Exploratory study of the moment capacity and semirigid moment-rotation behavior of round mortise and tenon joints," *Forest Products Journal* 58(7), 56-61.
- Gao, C., Wang, J., Yang, Q. S., and Yang, N. (2020). "Analysis of rocking behavior of Tang-Song timber frames under pulse-type excitations," *International Journal of Structural Stability and Dynamics* 20(1), Article ID 2050002. DOI: 10.1142/S0219455420500029
- Gao, Y., Tao, Z., Ye, L., Wang, D., and Zhang, L. (2015). "Low-cycle reversed loading tests study on typical mortise-tenon joints of traditional timber building based on friction mechanism," *Journal of Building Structures* 36(10), 139-145. DOI: 10.14006/j.jzjgxb.2015.10.017
- Guo, T., Yang, N., Zhou, H. B., and Wang, S. Y. (2021). "Experimental study on the moment-resisting performance of interior joints with wooden peg," CNKI, (<https://kns.cnki.net/kcms/detail/50.1218.TU.20210312.0953.006.html>), Accessed 01 April 2021.
- Han, X. L., Dai, J., Qian, W., and Li, B. L. (2020). "Effect of column foot tenon on behavior of larch column base joints based on concrete plinth," *BioResources* 15(3), 6648-6667. DOI: 10.15376/biores.15.3.6648-6667
- Huan, J. H., Ma, D. H., Guo, X. D., and Xu, S. (2019). "Experimental study of aseismic behaviors of flexural tenon joint, through tenon joint and dovetail joint reinforced with flat steel devices," *Journal of Beijing University of Technology* 4(8), 763-771. DOI: 10.11936/bjutxb2018010012
- Huang, H., Wu, Y. T., Li, Z., Sun, Z., and Chen, Z. (2018). "Seismic behavior of Chuan-Dou type timber frames," *Engineering Structures* 167, 725-739. DOI: 10.1016/j.engstruct.2017.10.072
- Johanides, M., Kubincova, L., Mikolasek, D., Lokaj, A., Sucharda, O., and Petr, M. (2021). "Analysis of rotational stiffness of the timber frame connection," *Sustainability* 13(1), 1-5. DOI: 10.3390/su13010156
- Li, S. C., Chen, L. K., Jiang, L. Z., and Li, J. Q. (2019). "Experimental investigation on the seismic behavior of the semi-rigid one-way straight mortise-tenon joint of a historical timber building," *International Journal of Architectural Heritage* 4(17), 1-13. DOI: 10.1080/15583058.2019.1587041
- Ma, H., Luan, X. Y., Li, Z. B., and Cui, H. J. (2019). "Seismic performance of damaged dovetail joints with different damaged degrees in timber frames," *Advances in Civil Engineering* 2019, Article ID 7238217. DOI: 10.1155/2019/7238217

- Meng, X. J., Li, T. Y., and Yang, Q. S. (2019). "Lateral structural performance of column frame layer and Dou-Gong layer in a timber structure," *KSCE Journal of Civil Engineering* 23(2), 666-677. DOI: 10.1007/s12205-018-0259-4
- Pan, Y., Tang, L. N., Wang, H. Q., and Yao, Y. (2014). "Investigation and analysis of damage to ancient buildings in Lushan M_s7.0 earthquake," *Earthquake Engineering and Engineering Dynamics* 34(1), 140-146. DOI: 10.13197/j.eeev.2014.01.140.pany.018
- Qu, Z., Fu, X., Kishiki, S., and Cui, Y. (2020). "Behavior of masonry infilled Chuandou timber frames subjected to in-plane cyclic loading," *Engineering Structures* 211, Article ID 110449. DOI: 10.1016/j.engstruct.2020.110449
- Sakata, H., Yamazaki, Y., Udagawa, H., and Ohashi, Y. (2012). "Experimental study on flexural-shear behavior of mortise-tenon joint with dowel," *J. Structural Construction Engineering (Transactions of AIJ)* 77(671), 45-54. DOI: 10.3130/aijs.77.45
- Sha, B., Wang, H., and Li, A. (2019). "The influence of the damage of mortise-tenon joint on the cyclic performance of the traditional Chinese timber frame," *Applied Sciences-Basel* 9(16), 3429-3449 DOI: 10.3390/app9163429
- Shi, X., Li, T., Chen, Y., Chen, J., and Yang, Q. (2020). "Full-scale tests on the horizontal hysteretic behavior of a single-span timber frame," *International Journal of Architectural Heritage* 14(3), 398-414. DOI: 10.1080/15583058.2018.1547799
- Song, X. S. (2014). *Experimental Study on Structural Performance and Reinforcement of Ancient Wooden Buildings*, Ph.D. Dissertation, Beijing University of Technology, Beijing, China.
- Su, H. H., Gao, Y. L., Tao, Z., Su, H. X., and Zhang, Q. (2020). "Tests for effects of lateral tenon and mortise tightness on aseismic performance of step through tenon joints," *Journal of Vibration and Shock* 39(15), 142-149. DOI: 10.13465/j.cnki.jvs.2020.15.019
- Sui, Y., Zhao, H. T., Xue, J. Y., and Xie, Q. F. (2010). "Experimental study on characteristics of mortise-tenon joints in historic timber buildings," *World Earthquake Engineering* 26(2), 88-92. DOI: 10.13031/2013.29857
- Wan, J., Yang, Q. S., Wei, J. W., and Li, T. Y. (2020). "Initial motion analysis of traditional Chinese rocking timber frame subjected to horizontal ground motion: Theoretical and numerical investigations," *Engineering Structures* 203, Article ID 109898. DOI: 10.1016/j.engstruct.2019.109898
- Xie, Q. F., Zheng, P. J., Cui, Y. Z., Qian, C. Y., and Zhang, F. L. (2015a). "Experimental study on seismic behavior of straight mortise-tenon joints of ancient timber buildings," *Earthquake Engineering and Engineering Dynamics* 35(3), 232-241. DOI: 10.13197/j.eeev.2015.03.232.xieqf.029
- Xie, Q. F., Du, B., Xiang, W., Zhang, P., and Zhang, F. (2015b). "Experimental study on seismic behavior and size effect of dovetail mortise-tenon joints of ancient timber buildings," *Journal of Building Structures* 36(3), 112-120. DOI: 10.14006/j.jzjgxb.2015.03.014
- Xie, Q. F., Tong, Y. Y., Zhang, L. P., Li, S. Y., and Wang, L. (2019). "Seismic behavior of Chinese traditional timber frames with masonry infill wall: Experimental tests and hysteretic model," *International Journal of Architectural Heritage* Online, Article ID 1665140. DOI: 10.1080/15583058.2019.1665140
- Xie, Q. F., Zhang, L. P., Miao, Z., and Zhou, W. J. (2020). "Lateral behavior of traditional Chinese timber-frames strengthened with shape-memory alloy:

- Experiments and analytical model,” *Journal of Structural Engineering* 146(6), Article ID 216220580. DOI: 10.1061/(ASCE)ST.1943-541X.0002583
- Xu, M. G., and Qiu, H. X. (2011). “Experimental study on seismic behavior of mortise-tenon joints of ancient architectures,” *Building Science* 7, 59-61. DOI: 10.13614/j.cnki.11-1962/tu.2011.07.019
- Xue, J. Y., Guo, R., Qi, L. J., and Xu, D. (2019). “Experimental study on the seismic performance of traditional timber mortise-tenon joints with different looseness under low-cyclic reversed loading,” *Advances in Structural Engineering* 22(6), 1312-1328. DOI: 10.1177/1369433218814167
- Yang, Q. S., He, J. X., and Wang, J. (2021). “Study on the mechanical behaviors of timber frame with the simplified column foot joints,” *Structural Engineering and Mechanics* 77(30), 383-394. DOI: 10.12989/sem.2021.77.3.383
- Zhang, X. C., Wu, C. W., Xue, J. Y., and Ma, H. (2019). “Fast nonlinear analysis of traditional Chinese timber-frame building with Dou-Gon,” *International Journal of Architectural Heritage* 14(8), 1252-1268. DOI: 10.1080/15583058.2019.1604847
- Zhang, X. C., Xue, J. Y., Zhao, H. T., and Sui, Y. (2011). “Experimental study on Chinese traditional timber-frame building by shaking table test,” *Structural Engineering and Mechanics* 40(4), 453-469. DOI: 10.12989/sem.2011.40.4.453
- Zhao, H. T., Dong, C. Y., Xue, J. Y., Yan, S., and Zhang, H. Y. (2010). “The experimental study on the characteristics of mortise-tenon joint historic timber buildings,” *Journal of Xi’an University of Architecture and Technology (Natural Science Edition)* 3, 16-19.
- Zhou, Q., and Yan, W. M. (2011). “Strengthening analysis on tenon-mortise joint of a face beam in Tai-He Palace in the Forbidden City in China,” *Advanced Materials Research* 255-260, 1597-1602, DOI: 10.4028/www.scientific.net/AMR.255-260.1597
- Zhou, Q., Yan, W. M., and Zhou, H. Y. (2010). “Stochastic seismic response of Chinese ancient wooden buildings,” *Journal of Wuhan University of Technology* 32(9), 125-128. DOI: 10.3963/j.issn.1671-4431.2010.09.027

Article submitted: April 1, 2021; Peer review completed: May 23, 2021; Revised version received and accepted: May 26, 2021; Published: June 7, 2021.
DOI: 10.15376/biores.16.3.5313-5328